Earth and Planetary Science Letters 489 (2018) 17–27

Contents lists available at ScienceDirect

Earth and Planetary Science Letters

www.elsevier.com/locate/epsl

Does permanent extensional deformation in lower forearc slopes indicate shallow plate-boundary rupture?

J. Geersen [a,*], C.R. Ranero [b,c], H. Kopp [a], J.H. Behrmann [a], D. Lange [a], I. Klaucke [a], S. Barrientos [d], J. Diaz-Naveas [e], U. Barckhausen [f], C. Reichert [f]

[a] GEOMAR Helmholtz Centre for Ocean Research Kiel, Wischhofstrasse 1-3, 24148 Kiel, Germany
[b] Barcelona Center for Subsurface Imaging, Instituto de Ciencias del Mar, CSIC, Passeig Maritim de la Barceloneta 37-49, 08003 Barcelona, Spain
[c] ICREA, Pg. Lluís Companys 23, 08010 Barcelona, Spain
[d] Centro Sismológico Nacional, Facultad de Ciencias Físicas y Matemáticas, Universidad de Chile, Blanco Encalada 2002, Santiago, Chile
[e] Escuela de Ciencias del Mar, Pontificia Universidad Católica de Valparaíso, Av. Altamirano 1480, Valparaíso, Chile
[f] Bundesanstalt für Geowissenschaften und Rohstoffe (BGR), Stilleweg 2, 30655 Hannover, Germany

ARTICLE INFO

Article history:
Received 13 December 2017
Received in revised form 23 February 2018
Accepted 23 February 2018
Available online 7 March 2018
Editor: P. Shearer

Keywords:
subduction-zone
marine forearc
seismic gap
Northern Chile
active tectonics
permanent deformation

ABSTRACT

Seismic rupture of the shallow plate-boundary can result in large tsunamis with tragic socio-economic consequences, as exemplified by the 2011 Tohoku-Oki earthquake. To better understand the processes involved in shallow earthquake rupture in seismic gaps (where megathrust earthquakes are expected), and investigate the tsunami hazard, it is important to assess whether the region experienced shallow earthquake rupture in the past. However, there are currently no established methods to elucidate whether a margin segment has repeatedly experienced shallow earthquake rupture, with the exception of mechanical studies on subducted fault-rocks. Here we combine new swath bathymetric data, unpublished seismic reflection images, and inter-seismic seismicity to evaluate if the pattern of permanent deformation in the marine forearc of the Northern Chile seismic gap allows inferences on past earthquake behavior. While the tectonic configuration of the middle and upper slope remains similar over hundreds of kilometers along the North Chilean margin, we document permanent extensional deformation of the lower slope localized to the region 20.8°S–22°S. Critical taper analyses, the comparison of permanent deformation to inter-seismic seismicity and plate-coupling models, as well as recent observations from other subduction-zones, including the area that ruptured during the 2011 Tohoku-Oki earthquake, suggest that the normal faults at the lower slope may have resulted from shallow, possibly near-trench breaking earthquake ruptures in the past. In the adjacent margin segments, the 1995 Antofagasta, 2007 Tocopilla, and 2014 Iquique earthquakes were limited to the middle and upper-slope and the terrestrial forearc, and so are upper-plate normal faults. Our findings suggest a seismo-tectonic segmentation of the North Chilean margin that seems to be stable over multiple earthquake cycles. If our interpretations are correct, they indicate a high tsunami hazard posed by the yet un-ruptured southern segment of the seismic gap.

1. Introduction

The disastrous 2011 Tohoku-Oki earthquake highlights the tremendous societal impact of a great subduction-zone earthquake and its associated tsunami on coastal communities. During the earthquake, unexpected large rupture of the shallow segment of the plate-boundary caused more than 50 m of seafloor displacement (Kodaira et al., 2012). This is considered to be the main cause for the devastating tsunami and demonstrates the need to improve our understanding of rupture processes in the shallowest parts of subduction zones. A key objective in this context is to identify similar seismo-tectonic segments where shallow earthquake rupture has occurred in the past (and therefore may happen in the future) by exploring the question if shallow earthquake rupture creates a diagnostic fingerprint of permanent deformation structures in the overriding forearc.

* Corresponding author.
E-mail addresses: jgeersen@geomar.de (J. Geersen), cranero@icm.csic.es (C.R. Ranero), hkopp@geomar.de (H. Kopp), jbehrmann@geomar.de (J.H. Behrmann), dlange@geomar.de (D. Lange), iklaucke@geomar.de (I. Klaucke), sbarrien@dgf.uchile.cl (S. Barrientos), juan.diaz@pucv.cl (J. Diaz-Naveas), udo.barckhausen@bgr.de (U. Barckhausen), christian.reichert@bgr.de (C. Reichert).

https://doi.org/10.1016/j.epsl.2018.02.030

Work on brittle deformation structures relating to seismogenesis shows that permanent deformation fabrics at core and outcrop scale can be diagnostic of different types of seismic rupture (Sibson, 1975; Fagereng, 2011; Vannucchi et al., 2017). At larger scale, studies have tried to relate deformation in the terrestrial forearc to variations in seismogenic behavior of the margin (Baker et al., 2013; Saillard et al., 2017). However, active faults onshore, clearly relating to co-seismic plate-boundary deformation are often difficult to detect and interpretation of paleoseismic records relies on correct dating of co-seismic deposits (e.g. tsunami layers). Furthermore, these structures are mostly far from the maxima of rupture of great and giant earthquakes, which are commonly located offshore. In the marine forearc above the zone of maximum earthquake slip, active fault scarps are in contrast often excellently preserved (Geersen et al., 2011). This has already been used to show that deformation of accretionary wedges can be related to the seismic behavior of the megathrust (Cubas et al., 2016) and that the structure and morphology of a marine forearc and the generation and activity of forearc faults is influenced by the seismogenic behavior of the megathrust (Cubas et al., 2013a, 2013b). With more high-resolution bathymetric data becoming available there is the opportunity to study the distribution of permanent upper-plate deformation structures in marine forearcs over large regions (thousands of square kilometers) and relate them to past earthquake behavior.

After 137 yrs of quiescence (Lomnitz, 2004), the North Chilean margin showed an increase in seismicity in early 2014, resulting in the Mw. 8.1 Iquique earthquake on 1 April 2014 (Fig. 1) (Hayes et al., 2014; Ruiz et al., 2014; Schurr et al., 2014). There was no major Pacific-wide tsunami, probably due to the fact that the coseismic rupture did not extend to the shallow plate-boundary near the trench axis. However, despite rupturing a ~150-km-long stretch of the margin, the earthquake left large areas of the so-called Northern Chile seismic gap untouched (Fig. 1). This gap to the south of the 2014 Iquique earthquake, to the north of the 1995 Antofagasta earthquake and updip of the 2007 Tocopilla earthquake (Fig. 1) still contains elastic strain accumulated since 1877, posing now a high seismic hazard due to stress transfer from the 2014 rupture (Hayes et al., 2014). Onshore GPS data further suggest a high degree of plate-coupling that may extend close to the trench (Béjar-Pizarro et al., 2013; Schurr et al., 2014; Métois et al., 2016). This leads to the timely question whether permanent deformation structures in this yet un-ruptured margin segment allow deducing the spatial distribution and updip limit of earthquake ruptures in the geological past.

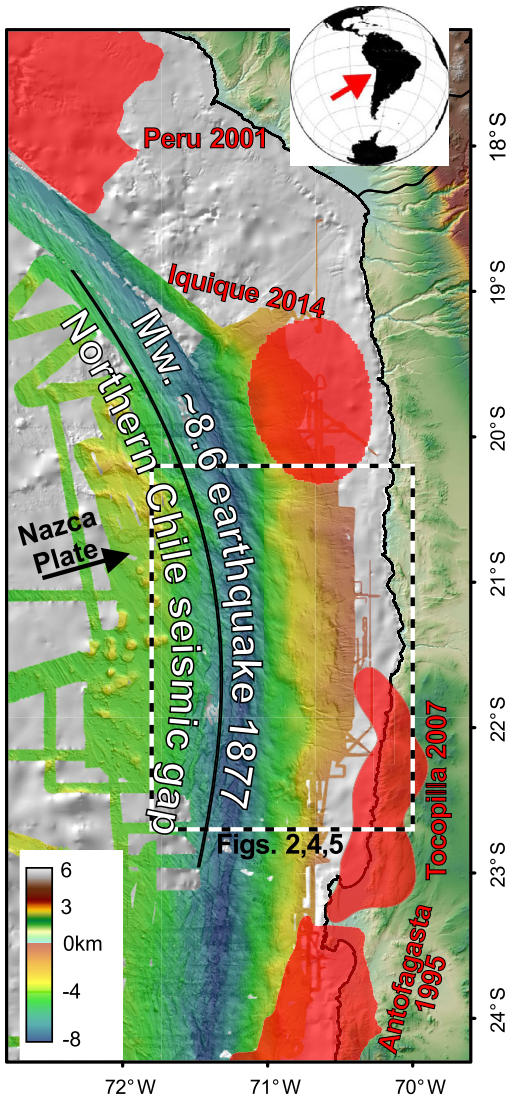

Fig. 1. Overview map of northern Chile and southern Peru. Swath bathymetric data from R/V SONNE Cruise 244 complemented with older data collected over the last two decades during multiple seagoing campaigns with German research vessels (R/V SONNE, R/V METEOR) and data from the Global Multi-Resolution Topography (GMRT) synthesis (Ryan et al., 2009). Shaded relief in the background is based on the GEBCO_08 Grid (version 20091120) data. Topographic data are taken from the Shuttle Radar Topography Mission (Farr et al., 2007). Red shaded regions are the co-seismic rupture areas of the 1995 Antofagasta (Pritchard et al., 2007), 2001 Peru (Pritchard et al., 2007), 2007 Tocopilla (Schurr et al., 2012), and 2014 Iquique (Schurr et al., 2014) earthquakes. (For interpretation of the colors in the figure(s), the reader is referred to the web version of this article.)

2. Data and methods

2.1. Swath bathymetry

Most of the swath bathymetric data used for this study were acquired during R/V SONNE cruise SO244 with a Kongsberg Maritime EM 122 multibeam echosounder operating at 12 kHz. During SONNE cruise SO244 the beam angle of the echosounder was set at 140°, except for a local survey on the outer rise and mid-slope region, where the beam angle was reduced to 120° in order to increase the resolution. The system was operated in dual-ping mode, where one beam is slightly tilted forward and the second ping slightly tiled towards the aft of the vessel. The pitch of the vessel was compensated automatically. Survey speed was 8 kn. Two CTD casts (conductivity, temperature, density probe) recorded water sound velocity profiles. A triangulation filter with three iterations was applied in order to eliminate outliers, and the sounding data were then cleaned manually for further elimination of erroneous soundings. The data were subsequently gridded using a near-neighbor algorithm that takes into account four neighboring cells, eliminates cells with less than two soundings per cell, and interpolates for two rows/columns. Below 3000 m water depth the surveyed area was gridded with a 75 m grid cell size. Sounding density in the upper slope region down to 3000 m water depth allowed griding at 50 m grid cell sizes. We complemented the high-resolution swath bathymetric data from SO244 with older data collected over the last two decades during multiple seagoing campaigns with German research vessels (R/V SONNE, R/V METEOR) and data from the Global Multi-Resolution Topography (GMRT) synthesis (Ryan et al., 2009).

2.2. Seismic reflection

Seismic reflection data off Northern Chile were collected by the German Bundesanstalt für Geowissenschaften und Rohstoffe (BGR) in 1995. The data were collected using R/V SONNE (cruise

SO104) in the framework of the crustal investigations off- and onshore Nazca/Central Andes (CINCA) project. The seismic signals were generated using a well-tuned, ~3,124-cubic-inch (51.2 l) air-gun array shot every 50 m. The data were recorded with a 3-km long digital streamer with 25 m group spacing.

Re-processing of seismic data with modern algorithms was conducted at the Barcelona Center for Subsurface Imaging (Barcelona-CSI) with the Claritas software package. After initial quality control and manual data editing, the seismic traces were cleaned with a pre-stack wavelet-shaping statistical deconvolution. Subsequently, shot point interpolation and offset regularization was conducted for two-dimensional filtering. Semblance-type velocity analyses were interpreted every 5 km. The water-layer multiple was attenuated with parabolic radon filtering on super gathers after normal-moveout correction with stacking velocities. A pre-stack time migration was done on receiver gathers with time and space varying velocities based on the velocity analysis. After pre-stack time migration, new velocity analyses were interpreted for common-mid-point stacking. After stacking, the data were post-stack time migrated using a finite difference algorithm, with velocity layer mimicking the large-scale seismic structure of the margin. For the shallow geology, seismic velocities were based on velocity analysis, whereas deeper in the section, seismic velocities were based on wide-angle seismic profiles across the margin (Contreras-Reyes et al., 2012). After post-stack time migration, the data were bandpass filtered with time- and space-varying frequencies, based on geological structure. For display purposes, the data are presented with an automatic gain control normalization based on the mean amplitude within a sliding window of 1 s.

2.3. Seismicity

To evaluate seismicity in the study area we use the earthquake catalog of the Centro Sismológico Nacional, Chile (CSN) for the years 2008–2013. Seismicity monitoring was carried out with a network of over 15 seismic stations located between 18°–23°S. Most stations were installed during the latter part of the last decade as a joint effort from the Deutsche GeoForschungsZentrum GFZ and the Institute de Physique du Globe de Paris (IPGP) under the framework of the Integrated Plate Boundary Observatory Chile (IPOC, www.ipoc-network.org). In addition to the IPOC stations, two stations from the permanent Chilean network (network codes C, C1) were used for earthquake detection and hypocenter location. Hypocenter locations are based on manually picked P and S wave arrivals, together with a local 1-D velocity model optimized for northern Chile with P-wave velocities increasing from 6.1 km/s at the surface to 8.4 km/s at 200 km depth.

3. Results

New high-quality swath bathymetric data collected in 2015 across the North Chilean marine forearc (Fig. 2), and unpublished re-processed seismic reflection images of the plate-boundary and upper-plate tectonic structure (Figs. 3 and 4) are used to derive the pattern of permanent deformation in the yet un-ruptured southern segment of the Northern Chile seismic gap between 20.3°S and 22.7°S. The deformation pattern is further set in relation to 6 years of regional seismicity (2008–2013) (Fig. 2B).

3.1. Permanent deformation structures in the marine forearc

The new seafloor map of the Northern Chile seismic gap to the south of the 2014 Iquique earthquake shows a complex structural pattern (Fig. 2). The upper continental slope (brownish colors in Fig. 2A) is dissected by steep (up to 35°), roughly N–S striking scarps (green lines in Fig. 2B) that vertically offset the seafloor up to 500 m. The scarps are the surface expressions of large seaward-dipping normal faults in the seismic data (Figs. 3 and 4). Upslope of these scarps a well-developed system of canyons and gullies, which are not intersected by major fault scarps, (blue lines in Fig. 2B) suggests relative tectonic stability in that region. Most of the upper-slope canyons terminate abruptly at the largest normal fault scarps. Here, canyon incision is outpaced by vertical displacement across the normal faults. This leads to sediment accumulation and filling of the canyon thalwegs in the hanging-wall thereby indicating the active nature of the faults. Yet further upslope the forearc is cut by landward-dipping normal faults imaged in the seismic data (e.g. km ~57 in Fig. 3B). These produce little seafloor relief in spite of considerable vertical offset of the top of the continental basement. Taken together, seaward and landward dipping normal faults on the upper slope outline prominent basement highs, which are identified from ~20.5°S all the way to Antofagasta Ridge south of Mejillones Peninsula at ~24°S (von Huene and Ranero, 2003). On the middle forearc slope (yellowish colors in Fig. 2A), structural features indicating stable sediment-dynamic conditions are less common and the density of N–S trending normal faults is much higher than on the upper slope. Vertical fault offsets are smaller on the middle forearc slope and expressed by seaward-dipping seafloor scarps that are some tens of meters high. South of ~22°S normal fault scarps seem less prominent on the middle forearc slope. Seismic line SO104-09 (Figs. 3B and 4) shows that this is due to a thin sediment cover. Normal faults that are active in this zone, however, create small offsets at the sediment-covered seafloor (Figs. 3B and 4). These observations show that the structure of the upper and middle forearc slope persists throughout the study area and over hundreds of kilometers along the margin.

Significant along-strike structural changes occur at the lower continental slope (green-bluish colors in Fig. 2A). North of 20.8°S and south of 22°S there is a fairly smooth morphology characterized by NW trending antiforms and synforms (purple lines in Fig. 2B) that have axes oriented roughly parallel to the oceanic spreading fabric (red dashed lines in Fig. 2B) on the oceanic Nazca Plate west of the deformation front. However, between 20.8°S and 22°S this structural fabric is overprinted by numerous seaward dipping normal fault scarps (km 29, 36 and 41 on seismic line SO104-07 in Fig. 3A) akin to those observed on the middle forearc slope. Here, normal faulting of the upper-plate extends to the area of the lower continental slope to within 5 km of the trench axis over a distance along the margin of about 100 km. This is not observed at other areas of the North Chilean subduction zone. Elsewhere, a frontal prism defines an area of contraction that is at least a few kilometers wide (von Huene and Ranero, 2003; Contreras-Reyes et al., 2014; Geersen et al., 2015). Seismic line SO104-09, located near the southern boundary of the extensional lower slope domain, has a 7-km-wide frontal sediment prism (Fig. 3B).

While large areas of the marine forearc are affected by extensional deformation, the seismic reflection lines (Fig. 3) do not fully resolve the depth extent of normal faulting. This could be due to a lack of structural continuity in the upper-plate, imaging complexity, or because the 3 km long streamer was too short to accurately image steep faults. Geersen et al. (2015) showed that the oceanic plate in the region carries a complex topography with large horst-and-grabens and seamounts. Once subducted, the topographic features may cause fracturing along the base of the upper-plate (Wang and Bilek, 2011). The forearc normal faults therefore likely penetrate into a network of fractures at depth, a structural setting which is usually not well resolved in 2D seismic data. The seismic lines, however, show that the normal faults are not limited to the shallow strata, as the top of the continental basement is often also offset at locations that project to the scarps at the seafloor

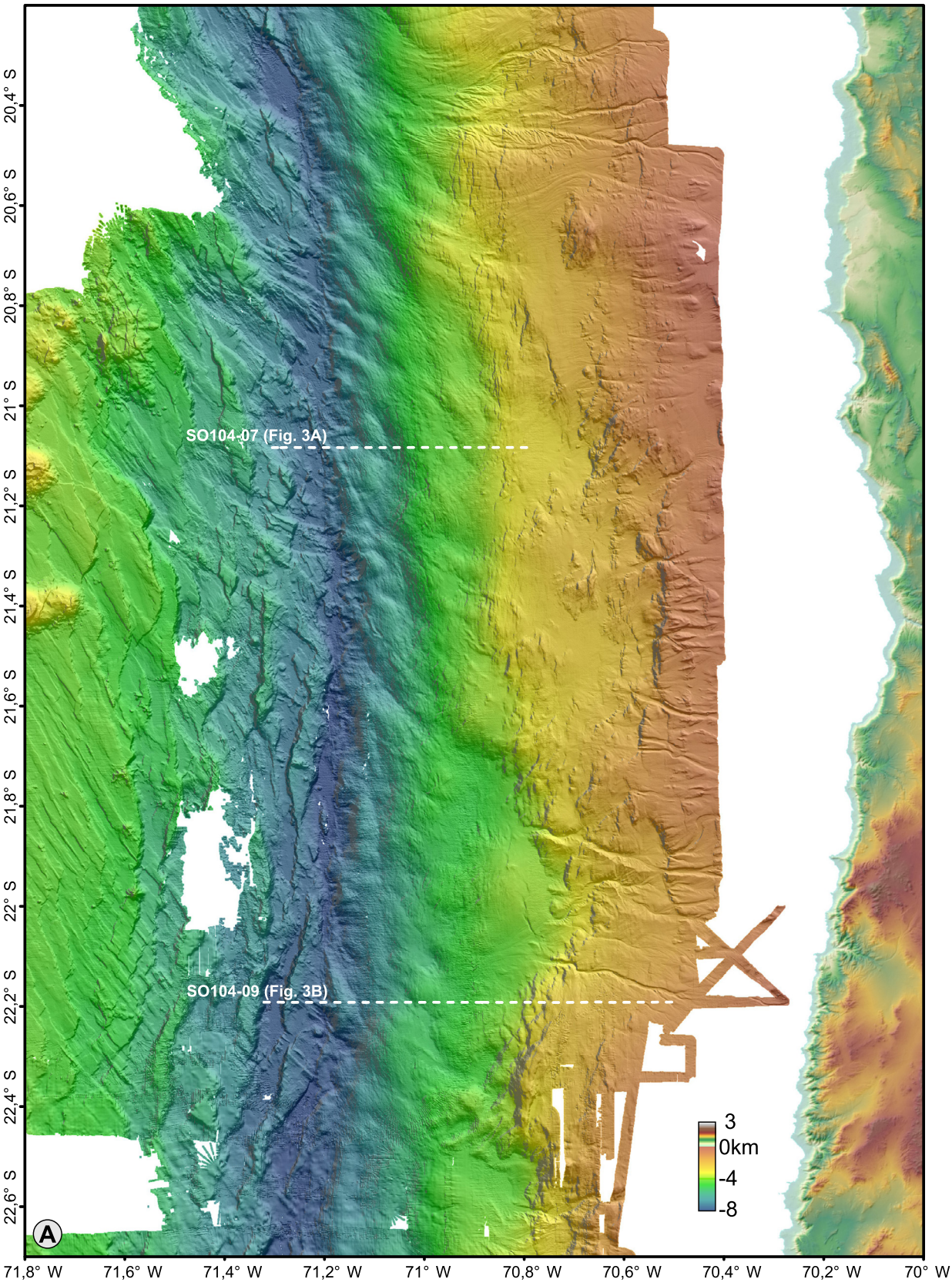

Fig. 2. Bathymetric and topographic map of the study area with tectonic interpretation. (A) Map view of swath bathymetric data collected during R/V SONNE cruises SO104 and SO244. Topographic data are taken from the Shuttle Radar Topography Mission (Farr et al., 2007). White dashed lines indicate the locations of the seismic data shown in Fig. 4. (B) Tectonic map of the marine forearc in the study area. Structural and tectonic interpretations as derived from the bathymetric data (Fig. 2A) and the seismic reflection images (Fig. 3). Grey shaded regions are the co-seismic rupture areas of the 2007 Tocopilla (Schurr et al., 2012) and 2014 Iquique (Schurr et al., 2014) earthquakes. Red contour lines are plate-coupling isolines (Schurr et al., 2014).

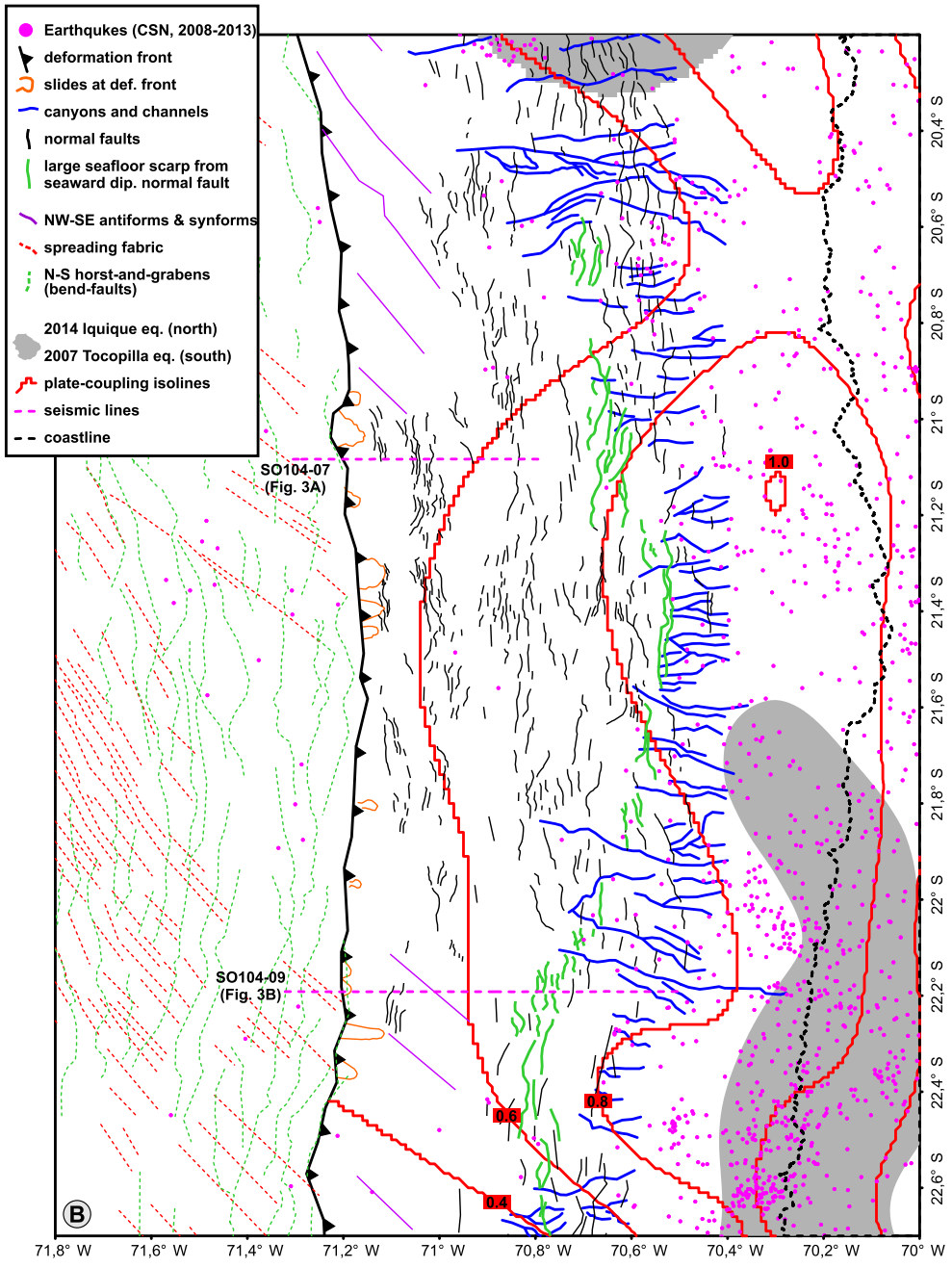

Fig. 2. (*continued*)

(Figs. 3–4). Along the erosional Central American margin, similar normal faults have been inferred to cut through the entire forearc, from the seafloor to the plate-boundary (Hensen et al., 2004; Ranero et al., 2008) and we consider it as likely that the normal faults in our study area extend to similar depths.

3.2. Seismicity in the marine forearc

The seismological catalog of the CSN includes 994 earthquakes in the study area (Fig. 2B) during the time period 01.01.2008–31.12.2013. Seismicity of this time period reflects interseismic deformation and was chosen in order to avoid a large bias from the foreshocks and aftershocks of the 2007 Tocopilla and 2014 Iquique earthquakes. The local magnitudes of the events are between Ml 1.4 and 5.8. The catalogue has a magnitude of completeness (Mc) of approximately 3.2 with little variations between the complete catalogue and the marine forearc. Because seismicity in the marine forearc is located outside of the seismological monitoring network located onshore, hypo-central depth are not well constrained, even though small magnitude earthquakes are detected (e.g. Fuenzalida et al., 2013). The spatial pattern of seismicity mimics the differences in forearc structure described above. Epicenter locations are concentrated onshore and in the area of the upper continental slope. Seaward of the large seaward-dipping seafloor scarps (green lines in Fig. 2B) seismicity is conspicuously absent in the zone between 20.8°S and 22.0°S, where normal faulting reaches close to the trench.

4. Discussion

Previous studies on the linkage between permanent deformation and great earthquakes have documented rupture to the

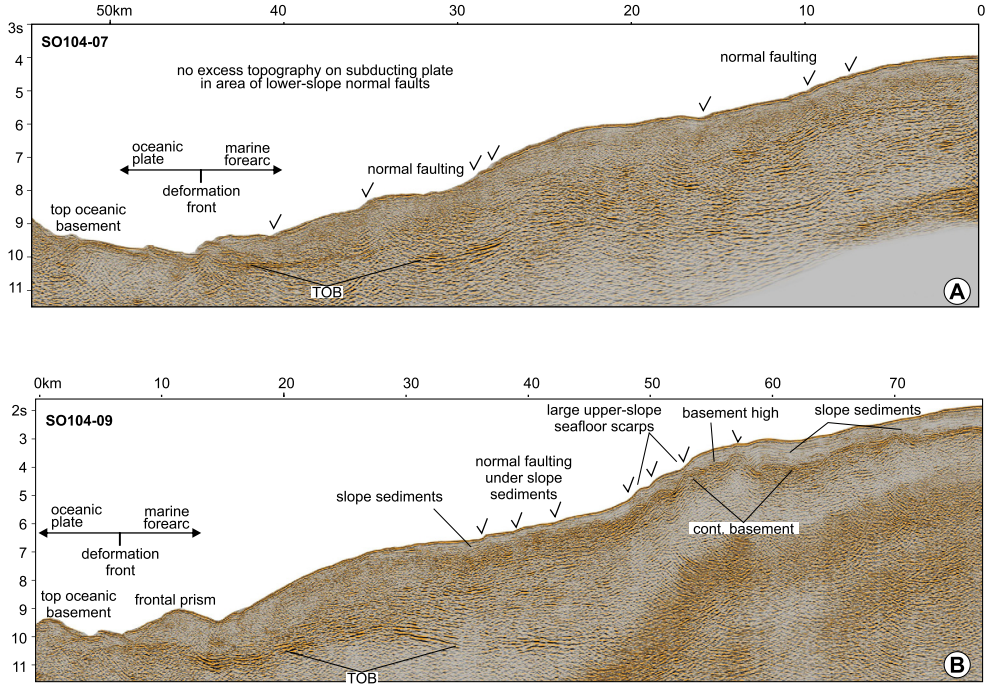

Fig. 3. Seismic reflection data. TOB = top oceanic basement. (A) Time section of seismic reflection line SO104-07. (B) Time section of seismic reflection line SO104-09.

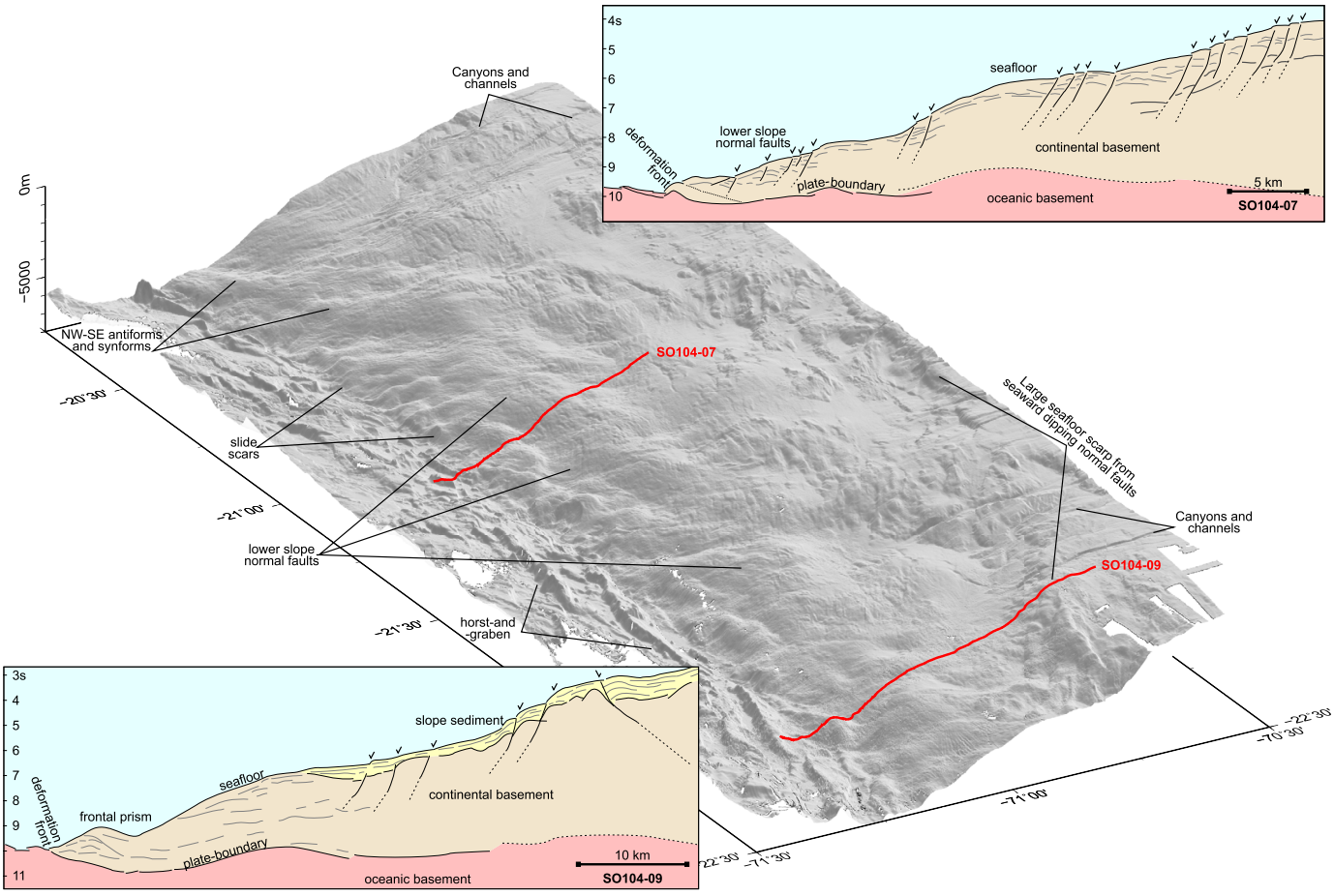

Fig. 4. Perspective view of the offshore North Chile forearc with interpretive line-drawings of the seismic reflection data (Fig. 3). The red lines indicate the locations of the seismic lines.

trench by comparing data from repeated geophysical surveys that were conducted before and after a great earthquake. This includes bathymetric and seismic imaging of the marine forearc and oceanic trench in the region of the 2011 Tohoku-Oki earthquake off northern Japan (Fujiwara et al., 2011; Kodaira et al., 2012) and the 2010 Maule earthquake in central Chile (Maksymowicz et al., 2017). However, these studies can only be conducted in regions where high-resolution geophysical data were collected before and after a great earthquake, basically limiting them to Japan and Chile. In areas where great earthquakes have not ruptured recently, but may likely occur in the future (seismic gaps) regional comparative studies of permanent deformation covering large areas, seismic coupling and historical seismicity have not been attempted for a seismic gap region prior to an anticipated large earthquake. In Northern Chile, upper-plate normal faults are mapped from the onshore forearc (Allmendinger and González, 2010) to near the slope toe (this study, Figs. 2B, 3A, and 4). Since normal faulting represents the most pervasive structural element of the North Chilean continental margin, their distribution may hold information on the spatial extent of seismic rupture during past megathrust earthquakes (Cubas et al., 2013a, 2013b). In the following we link permanent extensional deformation in the marine forearc, regional seismicity, inter-seismic plate-coupling (Béjar-Pizarro et al., 2013; Schurr et al., 2014; Métois et al., 2016), and critical wedge calculations in order to evaluate the possible occurrence of shallow earthquake rupture in the Northern Chile seismic gap during past earthquakes.

4.1. Linking permanent deformation to the seismic cycle and earthquake rupture

Along the upper continental slope, comparatively stable seafloor morphology (as expressed in the presence of long lived sediment transport features) and large vertical fault offsets indicate that permanent extensional deformation is concentrated along a few long-lived structures. Margin-wide high plate-coupling (>0.6) and the nucleation of great plate-boundary earthquakes (1995 Antofagasta, 2007 Tocopilla, 2014 Iquique) indicate the presence of a coherent 20–35 km thick upper-plate (Contreras-Reyes et al., 2012) from the coastal regions to the upper slope, capable of accumulating elastic energy, leading to large earthquakes. A thinner elastic plate, but possibly still capable of accumulating energy, exists under the mid-slope region, where the height of the normal fault scarps at the seafloor is <100 m but the overall number of faults increases. Even though faulting diminishes the structural integrity of the upper plate, the clear configuration of the faults, running in groups parallel to the margin (Fig. 2B), implies that a certain amount of elastic strength is maintained in this segment of the upper plate.

While the upper and the middle slope of the study area do not show significant along-strike changes in terms of extensional faulting, the lower slope shows different patterns. North of 20.8°S (in the area that ruptured during the 2014 Iquique earthquake) and south of 22°S (in the 1995 Antofagasta and 2007 Tocopilla rupture areas) broad NW trending antiforms and synforms characterize a fairly smooth lower slope morphology (purple lines, Fig. 2B). The smooth and featureless lower slope segments spatially correlate to regions of reduced inter-plate coupling (Figs. 2B and 5). Here, the shallow plate-boundary may contain an enhanced fluid abundance that will locally increase the areas with high fluid-pressure therewith counteracting the effective stress and reducing the plate-coupling. The relative abundance of fluids (and associated high fluid pressure) is supported by the reflective plate boundary in seismic images (Geersen et al., 2015), typically detected in the region of subducting sediment de-hydration (Ranero et al., 2008). Alternatively, the plate-boundary and the upper plate might be intensely deformed and fractured, perhaps related to the under-thrusting of ocean-plate relief (Wang and Bilek, 2011; Geersen et al., 2015). As a consequence, the forearc is largely made of incoherent material and may therefore accommodate most of the plate convergence by a combination of creep on the plate boundary and internal deformation of the upper-plate as expressed by the NW–SE trending antiforms and synforms. This interpretation is supported by the limited updip extent of the 1995, 2007, and 2014 earthquake rupture areas. These earthquakes rupture areas were constrained to under the middle and upper continental slope and/or the onshore forearc, and did not extend below the lower slope (Pritchard et al., 2007; Schurr et al., 2012, 2014).

In-between the smooth lower-slope segments (20.8°S–22°S), a well-developed system of normal faults extends across the lower slope to ∼5 km of the deformation front (Figs. 2B, 3A, and 4) and thus farther seaward than elsewhere along the entire Chilean subduction-zone (von Huene and Ranero, 2003; Geersen et al., 2011, 2015; Contreras-Reyes et al., 2014). After the giant 2010 Maule and 2011 Tohoku-Oki earthquakes, normal faulting aftershocks occurred in the overriding plates (Asano et al., 2011; Farias et al., 2011; Ide et al., 2011) in both, marine and terrestrial forearc regions. Furthermore, normal faults were seismically imaged and their seafloor scarps visually observed in the marine forearcs (Geersen et al., 2011, 2016; Tsuji et al., 2013).

Coulomb stress calculations for different subduction-zones showed that large plate-boundary earthquakes favor normal faulting in the overriding forearc in the co-seismic and early post-seismic phase (Farias et al., 2011; Toda et al., 2011; Aron et al., 2013; Geersen et al., 2016). The spatial extent of the zone of extension does, however, dependent on the exact co-seismic slip distribution (Aron et al., 2013). In addition, dynamic weakening of the plate-boundary during a large earthquake may move a forearc wedge into an extensional stress-regime therewith also supporting normal faulting in the co-seismic and early post-seismic phase (Wang et al., 2010; Schurr et al., 2012; Cubas et al., 2013a, 2013b).

Subduction of large relief of the oceanic plate such as seamounts or basement ridges could serve as an alternative explanation for the origin of the normal faults at the lower continental slope. However, several structural, tectonic, and seismological characteristics generally accompany subducting seamounts, including a re-entrant embayment and the combination of landward and seaward dipping normal faults (Masson et al., 1990; Ranero and von Huene, 2000) as well as earthquakes that cluster around the linear projection of the subducting seamount (e.g. Ranero and von Huene, 2000; Lange et al., 2016). None of these elements is observed at the extensional lower slope domain (20.8°S–22°S), nor is any large topography on the subducting oceanic plate under the lower slope (Fig. 3A). This lends support to the interpretation that the lower slope normal faults have been growing by repeated earthquakes, possibly involving rupture of the shallow plate-boundary.

4.2. Plate coupling and seismicity in the area of the lower slope normal faults

Different models of inter-seismic plate-coupling for the North Chilean margin have been recently computed (Béjar-Pizarro et al., 2013; Schurr et al., 2014; Métois et al., 2016) which share many similar features (Fig. 5). All models resolve a highly coupled patch (coupling = 0.8–1.0) between ∼20.6°S–22.6°S that extends from the coastal region to the middle continental slope. Farther seaward, coupling varies between 0.2–1.0 (Béjar-Pizarro et al., 2013), 0.5–0.7 (Schurr et al., 2014), and 0.2–0.6 (Métois et al., 2016). However, coupling in the very shallow part of the plate-boundary is not well resolved in the coupling models (e.g. Métois et al., 2016) and mostly depends on how boundary conditions are defined at the seaward side of the subduction-zone.

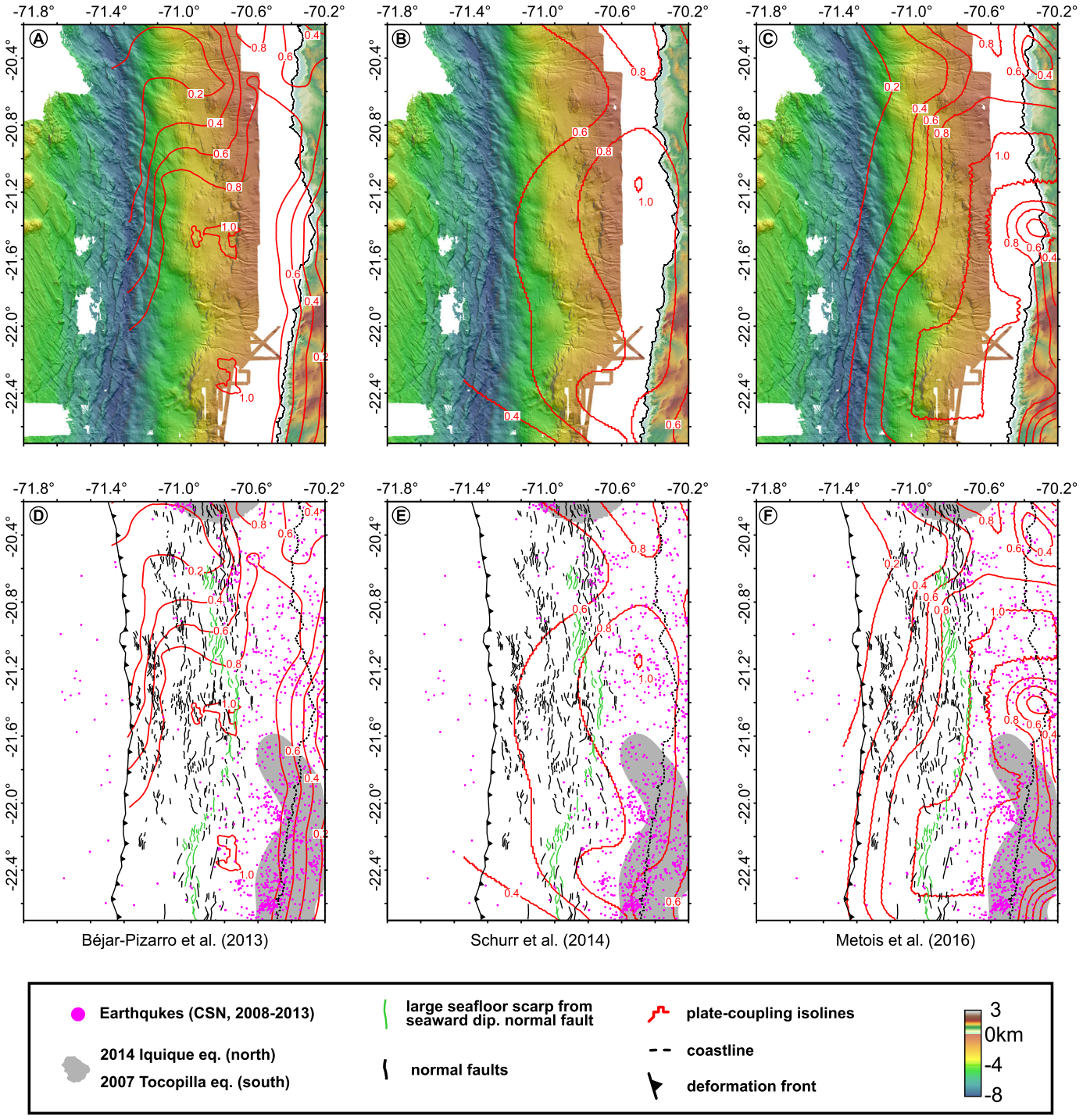

Fig. 5. Comparison of different plate-coupling models. Red lines are plate-coupling isolines (Béjar-Pizarro et al., 2013; Schurr et al., 2014; Métois et al., 2016). (A–C) Bathymetric and topographic map of the study area with plate-coupling. (D–F) Tectonic map of the marine forearc in the study area concentrating on permanent extensional deformation features (simplified from Fig. 2B). Grey shaded regions are the co-seismic rupture areas of the 2007 Tocopilla (Schurr et al., 2012) and 2014 Iquique (Schurr et al., 2014) earthquakes.

Spatial variations in plate-coupling partly correlate with variations in seismicity recorded over the time period 2008–2013 (Figs. 2B, 5D–5F). The upper slope and the terrestrial forearc, located above and landward of maximum plate-coupling, show a high inter-seismic activity. During the inter-seismic phase seismicity may mimic spatial changes in plate-coupling (Holtkamp and Brudzinski, 2014). This could well explain the high seismic activity under the upper slope and the terrestrial forearc which are located within the area of landward decreasing plate-coupling. The landward decrease in plate-coupling is likely a robust feature due to the proximity of the terrestrial GPS stations (Métois et al., 2016).

The situation is different under the middle and lower slope. Here, seismicity has been conspicuously absent in the region of the lower slope normal faults (20.8°S–22°S; Figs. 2B, 5D–5F). One reason for this lack of seismicity could be aseismic fault creep. However, in this case we would expect seismicity to occur between the highly coupled patch under the upper slope and the creeping lower slope segment. Alternatively, the lack of seismicity under the lower slope normal faults may result from the fact that

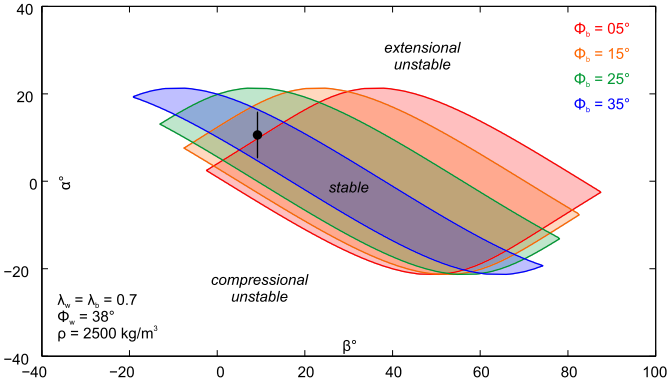

Fig. 6. Mechanical analysis of the wedge underlying the lower continental slope between the deformation front and the 5000 m depth contour-line. Critical envelopes are calculated for different basal friction angles. The shaded areas within the envelopes characterize stable regimes whereas the areas above and below characterize unstable extensional and compressional regimes respectively. The black dot characterizes the wedge in the area of the lower slope normal faults in α (seafloor slope) and β (dip of plate-boundary) space with $\sigma = 1$ for seafloor slope.

the plate-boundary in this region is not creeping, but locked, accumulating elastic deformation in the forearc, possibly all the way to the trench (Gagnon et al., 2005).

The comparison of the pattern of inter-seismic seismicity and models of plate-coupling does not allow direct conclusions on the behavior of past megathrust earthquakes. However, high plate-coupling at the latitudes of the lower slope normal faults in combination with 137 yrs of seismic quiescence (Lomnitz, 2004) in a region where past great earthquakes have occurred, indicates that the area may well host a large plate-boundary earthquake in the future. If seismo-tectonic segments are stable features over multiple earthquake cycles, as suggested by recent studies (e.g. Victor et al., 2011; Aron et al., 2013; Baker et al., 2013; Saillard et al., 2017), the margin segment at the latitudes of the lower slope normal faults likely also experienced large plate-boundary earthquakes in the past. In this context, the lower slope normal faults indicate that some of these past ruptures may have ruptured updip to the shallow plate-boundary.

4.3. Mechanical instability of the lower forearc

In order to investigate if stress changes during the earthquake cycle (Wang and Hu, 2006) may have caused permanent extensional deformation of the lower slope, we analyze the mechanical behavior of the wedge beneath the lower forearc slope. We use the critical wedge theory to evaluate the forerac wedge stability there as a function of α (seafloor slope) and β (dip angle of plate-boundary) using the analytical solutions by Dahlen et al. (1984). To constrain the wedge shape in α and β space (black dot in Fig. 6) we use 9° for the dip of the plate-boundary (β), taken from a nearby wide-angle seismic profile (Contreras-Reyes et al., 2012). Average seafloor slope (α) is derived from the bathymetric data between the deformation front and the 5000 m contour line, excluding landward (0°–180°) dipping areas. Seaward seafloor slope is separately determined for the northern (20.2°S–20.8°S) and southern (22°S–22.7°S) margin segments, where the lower slope is not affected by normal faulting, and for the area of the lower slope normal faults in-between (20.8°S–22°S). The resulting average slope values are 10.0° (±4.5°) in the northern segment, 9.6° (±5.7°) in the southern segment, and 10.6° (±5.2°) in the area of the lower slope normal faults.

We modeled a mechanically homogeneous and cohesionless wedge with an internal friction angle $\Phi w = 38°$ and density $\rho = 2500$ kg/m^3. We further use a pore-fluid pressure $\lambda = 0.7$ (as estimated for the wedge in the region of the 2011 Tohoku-Oki earthquake; Cubas et al., 2013a) within the wedge and at its base. The chosen value of $\lambda = 0.7$ is slightly lower as the regional estimate of 0.81 provided by Lamb (2006). However, the here documented pervasive faulting of the marine forearc, which likely provides vertical fluid conduits, argues against highly elevated pore fluid pressure. The basal friction angle Φw is then varied between 35° (3° smaller than within the wedge) to 5° in order to test which condition brings the wedge to extensional failure (Fig. 6). While the area within the envelopes characterizes mechanically stable states, implying that the wedge can slide along the plate-boundary without being deformed, the areas above and below characterize in-stable extensional and compressional regimes, respectively.

For a ratio of pore-fluid and overburden pressures $\lambda = 0.7$ the wedge is stable for most friction angles normally attributed to fault rocks (Byerlee, 1978). For the lower forearc wedge to become extensionally instable, the angle of basal friction has to be lowered to 5°. This value is similar to what has been proposed for the rocks in the shallow rupture area of the 2011 Tohoku-Oki earthquake (Fulton et al., 2013; Ujiie et al., 2013). We thus infer that the North Chilean plate-boundary under the outermost part of the forearc, in the area of the lower slope normal faults, does not exhibit a velocity strengthening behavior as suggested in the conceptual model of Wang and Hu (2006). It is either weak throughout the earthquake cycle (e.g. Gao and Wang, 2014), or it may weaken dynamically during a large earthquake by a fault weakening mechanism (Cubas et al., 2013a; Noda and Lapusta, 2013). A key observation in this context is the restriction of the lower slope normal faults to the area 20.8°S–22°S. This holds true even though the average slope gradient in the area of the lower slope normal faults (10.6°) is not much higher compared to the adjacent regions to the north (10.0°) and south (9.6°) not affected by normal faulting.

None of the structural and tectonic parameters that characterize the North Chilean margin (convergence rate and direction, trench sediment fill, oceanic plate-age and topography, nature of the upper-plate) shows latitudinal variations that could explain the spatial limitations of the lower slope normal faults. Based on this, and keeping in mind the latitudinal high plate-coupling and the lack of inter-seismic seismicity in the middle and lower slope region, we consider repeated shallow earthquake rupture as a likely cause for cumulative deformation leading to permanent extensional deformation of the lower slope (20.8°S–22°S) in the non-ruptured southern segment of the Northern Chile seismic gap.

4.4. Conceptual model

Previous studies suggest that seismic rupture of the plate-boundary (I) dynamically lowers the basal friction, which may bring the forearc wedge to extensional failure (Wang et al., 2010; Schurr et al., 2012; Cubas et al., 2013a, 2013b), and (II) induces a positive Coulomb stress change (Farias et al., 2011; Toda et al., 2011; Aron et al., 2013; Geersen et al., 2016). Based on our observations, mechanical calculations, and the comparison to models of inter-seismic plate-coupling and distribution of seismicity we develop a conceptual model relating the normal faults at the lower slope in the area 20.8°S–22°S to repeated shallow, possibly trench-breaking, seismic rupture, over multiple earthquake cycles (Fig. 7). In-line with previous studies (e.g. Victor et al., 2011) our results indicate a segmentation of the North Chilean margin into multiple long-living seismic segments, which however may also rupture in a single event as it likely happened during the 1877 earthquake.

A detailed study of forearc faults has been conducted at Mejillones Peninsula, where large faults cutting the continental shelf crop out at the surface and thus can be studied at outcrop scale. Shirzaei et al. (2012) used InSAR data to analyze the response of those forearc faults to rupture of the underlying plate-boundary. In their study, which covers a time-span of five years (2003–2008),

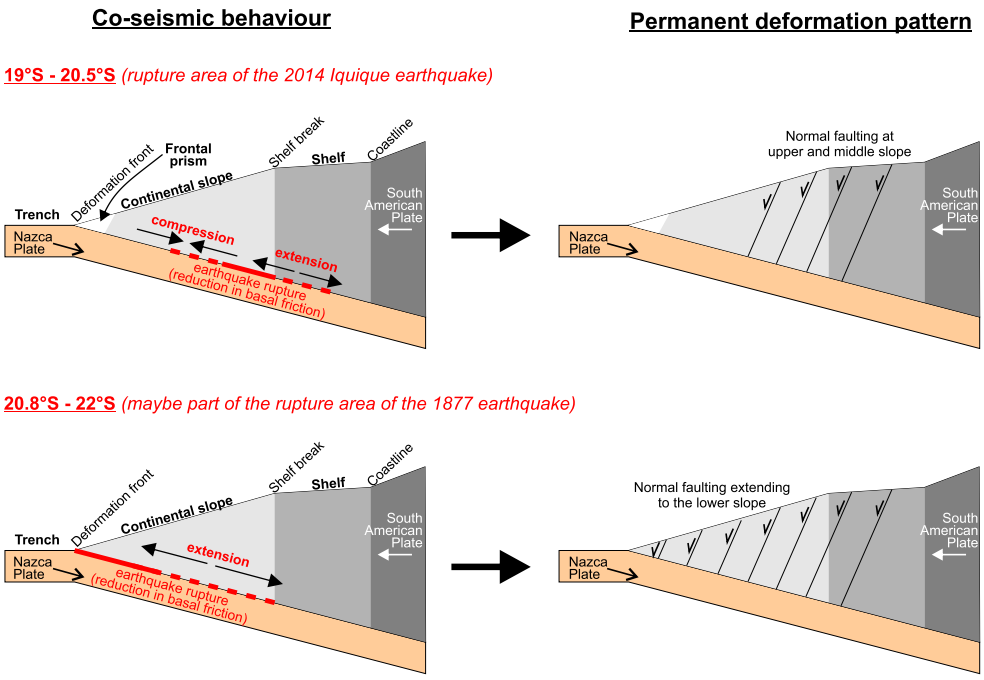

Fig. 7. Conceptual model linking lower slope normal faulting off Northern Chile to seismic rupture of the underlying shallow plate-boundary.

they document two closely spaced faults which changed their sense of slip relative to the 2007 Tocopilla earthquake (compare Fig. 1 for location). This implies that the slip history of the marine forearc normal faults discussed in this study might be more complex than sketched in the conceptual model. However, over many earthquake cycles their normal faulting component dominates (i.e. the hanging-wall has moved downward with respect to the foot-wall). If time-series for submerged forearc faults will become available at some point (e.g. through seafloor geodesy) this will help to understand temporal changes in fault behavior in relation to seismogenesis. Until then, the detailed documentation of permanent deformation might be the best proxy to infer seismogenic behavior over long time-scales (many earthquake cycles).

5. Conclusions

We bathymetrically mapped and seismically imaged the marine forearc of the Northern Chile seismic gap in an attempt to study the potential relationships between past earthquake rupture and permanent upper-plate deformation. While the structural character of the middle and upper slope remains similar throughout the region, we document permanent extensional deformation of the lower slope localized to the region 20.8°S–22°S. Repeated shallow earthquake rupture seems the most likely cause for the origin of lower slope extension, indicating that permanent upper-plate deformation may be a proxy to study past earthquake behavior. The yet un-ruptured southern segment of the Northern Chile seismic gap consequently poses a high tsunami hazard, especially in the light of possible stress transfer from the nearby 2014 Iquique earthquake.

Acknowledgements

Jacob Geersen was funded by a grant (CP1404) of the Cluster of Excellence 80 'The Future Ocean', funded within the framework of the Excellence Initiative by Deutsche Forschungsgemeinschaft (DFG) on behalf of the German federal and state governments. César R. Ranero was supported by the Grup de Recerca 2014SGR940 de la Generalitat de Catalunya. R/V SONNE Cruises SO-104 (Grant No. 03G104A) and SO-244 (Grant No. 03G0244A) were supported by the German Bundesministerium für Bildung und Forschung (BMBF). We thank Nadaya Cubas for providing the script for the critical taper analysis and Willi Weinrebe for help with the perspective map shown in Fig. 4. Seismic reflection data were collected by the BGR and re-processed at the Barcelona Center for Subsurface Imaging. We thank Ivan Vargas and Alcinoe Calahorrano for their processing work. Nina Kukowski and an anonymous reviewer are acknowledged for their comments and suggestions which helped us to improve the manuscript.

References

Allmendinger, R.W., González, G., 2010. Invited review paper: Neogene to Quaternary tectonics of the coastal Cordillera, northern Chile. Tectonophysics 495, 93–110. https://doi.org/10.1016/j.tecto.2009.04.019.

Aron, F., Allmendinger, R.W., Cembrano, J., González, G., Yáñez, G., 2013. Permanent fore-arc extension and seismic segmentation: insights from the 2010 Maule earthquake, Chile. J. Geophys. Res., Solid Earth 118, 724–739. https://doi.org/10.1029/2012JB009339.

Asano, Y., Saito, T., Ito, Y., Shiomi, K., Hirose, H., Matsumoto, T., Aoi, S., Hori, S., Sekiguchi, S., 2011. Spatial distribution and focal mechanisms of aftershocks of the 2011 off the Pacific coast of Tohoku Earthquake. Earth Planets Space 63, 29. https://doi.org/10.5047/eps.2011.06.016.

Baker, A., Allmendinger, R.W., Owen, L.A., Rech, J.A., 2013. Permanent deformation caused by subduction earthquakes in northern Chile. Nat. Geosci. 6, 492–496. https://doi.org/10.1038/ngeo1789.

Béjar-Pizarro, M., Socquet, A., Armijo, R., Carrizo, D., Genrich, J., Simons, M., 2013. Andean structural control on interseismic coupling in the North Chile subduction zone. Nat. Geosci. 6, 462–467. https://doi.org/10.1038/ngeo1802.

Byerlee, J., 1978. Friction of rocks. Pure Appl. Geophys. 116 (4), 615–626. https://doi.org/10.1007/BF00876528.

Contreras-Reyes, E., Becerra, J., Kopp, H., Reichert, C., Díaz-Naveas, J., 2014. Seismic structure of the north-central Chilean convergent margin: subduction erosion of a paleomagmatic arc. Geophys. Res. Lett. 41, 2013GL058729. https://doi.org/10.1002/2013GL058729.

Contreras-Reyes, E., Jara, J., Grevemeyer, I., Ruiz, S., Carrizo, D., 2012. Abrupt change in the dip of the subducting plate beneath north Chile. Nat. Geosci. 5, 342–345.

Cubas, N., Avouac, J.P., Leroy, Y.M., Pons, A., 2013a. Low friction along the high slip patch of the 2011 Mw 9.0 Tohoku-Oki earthquake required from the wedge structure and extensional splay faults. Geophys. Res. Lett. 40, 4231–4237. https://doi.org/10.1002/grl.50682.

Cubas, N., Avouac, J.-P., Souloumiac, P., Leroy, Y., 2013b. Megathrust friction determined from mechanical analysis of the forearc in the Maule earthquake area. Earth Planet. Sci. Lett. 381, 92–103. https://doi.org/10.1016/j.epsl.2013.07.037.

Cubas, N., Souloumiac, P., Singh, S.C., 2016. Relationship link between landward vergence in accretionary prisms and tsunami generation. Geology 44 (10), 787–790. https://doi.org/10.1130/G38019.1.

Dahlen, F.A., Suppe, J., Davis, D., 1984. Mechanics of fold-and-thrust belts and accretionary wedges: cohesive Coulomb theory. J. Geophys. Res., Solid Earth 89 (B12), 10087–10101. https://doi.org/10.1029/JB088iB02p01153.

Fagereng, Å., 2011. Geology of the seismogenic subduction thrust interface. Geol. Soc. (Lond.) Spec. Publ. 359, 55–76. https://doi.org/10.1144/SP359.4.

Farías, M., Comte, D., Roecker, S., Carrizo, D., Pardo, M., 2011. Crustal extensional faulting triggered by the 2010 Chilean earthquake: the Pichilemu seismic sequence. Tectonics 30, TC6010. https://doi.org/10.1029/2011TC002888.

Farr, T.G., Rosen, P.A., Caro, E., Crippen, R., Duren, R., Hensley, S., Kobrick, M., Paller, M., Rodriguez, E., Roth, L., Seal, D., Shaffer, S., Shimada, J., Umland, J., Werner, M., Oskin, M., Burbank, D., Alsdorf, D., 2007. The shuttle radar topography mission. Rev. Geophys. 45, RG2004. https://doi.org/10.1029/2005RG000183.

Fuenzalida, A., Schurr, B., Lancieri, M., Sobiesiak, M., Madariaga, R., 2013. High-resolution relocation and mechanism of aftershocks of the 2007 Tocopilla (Chile) earthquake. Geophys. J. Int. 194 (2), 1216–1228. https://doi.org/10.1093/gji/ggt163.

Fujiwara, T., Kodaira, S., No, T., Kaiho, Y., Takahashi, N., Kaneda, Y., 2011. The 2011 Tohoku-Oki Earthquake: displacement reaching the trench axis. Science 334, 1240.

Fulton, P.M., Brodsky, E.E., Kano, Y., Mori, J., Chester, F., Ishikawa, T., Expedition 343, 343t, 2013. Low coseismic friction on the Tohoku-Oki fault determined from temperature measurements. Science 342 (6163), 1214–1217. https://doi.org/10.1126/science.1243641.

Gagnon, K., Chadwell, C.D., Norabuena, E., 2005. Measuring the onset of locking in the Peru–Chile trench with GPS and acoustic measurements. Nature 434, 205–208. https://doi.org/10.1038/nature03412.

Gao, X., Wang, K., 2014. Strength of stick-slip and creeping subduction megathrusts from heat flow observations. Science 345 (6200), 1038–1041. https://doi.org/10.1126/science.1255487.

Geersen, J., Behrmann, J.H., Völker, D., Krastel, S., Ranero, C.R., Diaz-Naveas, J., Weinrebe, W., 2011. Active tectonics of the South Chilean marine fore arc (35°S–40°S). Tectonics 30, TC3006. https://doi.org/10.1029/2010TC002777.

Geersen, J., Ranero, C.R., Barckhausen, U., Reichert, C., 2015. Subducting seamounts control interplate coupling and seismic rupture in the 2014 Iquique earthquake area. Nat. Commun. 6, 8267. https://doi.org/10.1038/ncomms9267.

Geersen, J., Scholz, F., Linke, P., Schmidt, M., Lange, D., Behrmann, J.H., Völker, D., Hensen, C., 2016. Fault zone controlled seafloor methane seepage in the rupture area of the 2010 Maule earthquake, Central Chile. Geochem. Geophys. Geosyst. 17, 4802–4813. https://doi.org/10.1002/2016GC006498.

Hayes, G.P., Herman, M.W., Barnhart, W.D., Furlong, K.P., Riquelme, S., Benz, H.M., Bergman, E., Barrientos, S., Earle, P.S., Samsonov, S., 2014. Continuing megathrust earthquake potential in Chile after the 2014 Iquique earthquake. Nature 512, 295–298. https://doi.org/10.1038/nature13677.

Hensen, C., Wallmann, K., Schmidt, M., Ranero, C.R., Suess, E., 2004. Fluid expulsion related to mud extrusion off Costa Rica—a window to the subducting slab. Geology 32 (3), 201–204.

Holtkamp, S., Brudzinski, M.R., 2014. Megathrust earthquake swarms indicate frictional changes which delimit large earthquake ruptures. Earth Planet. Sci. Lett. 390, 234–243. https://doi.org/10.1016/j.epsl.2013.10.033.

Ide, S., Baltay, A., Beroza, G.C., 2011. Shallow dynamic overshoot and energetic deep rupture in the 2011 Mw 9.0 Tohoku-Oki earthquake. Science 332, 1426–1429. https://doi.org/10.1126/science.1207020.

Kodaira, S., No, T., Nakamura, Y., Fujiwara, T., Kaiho, Y., Miura, S., Takahashi, N., Kaneda, Y., Taira, A., 2012. Coseismic fault rupture at the trench axis during the 2011 Tohoku-Oki earthquake. Nat. Geosci. 5, 646–650.

Lamb, S., 2006. Shear stresses on megathrusts: implications for mountain building behind subduction zones. J. Geophys. Res., Solid Earth 111 (B7), B07401. https://doi.org/10.1029/2005JB003916.

Lange, D., Geersen, J., Barrientos, S., Moreno, M., Grevemeyer, I., Contreras-Reyes, E., Kopp, H., 2016. Aftershock seismicity and tectonic setting of the 2015 September 16 Mw 8.3 Illapel earthquake, Central Chile. Geophys. J. Int. 206, 1424–1430. https://doi.org/10.1093/gji/ggw218.

Lomnitz, C., 2004. Major earthquakes of Chile: a historical survey, 1535–1960. Seismol. Res. Lett. 75, 368–378. https://doi.org/10.1785/gssrl.75.3.368.

Maksymowicz, A., Chadwell, C.D., Ruiz, J., Tréhu, A.M., Contreras-Reyes, E., Weinrebe, W., Díaz-Naveas, J., Gibson, J.C., Lonsdale, P., Tryon, M.D., 2017. Coseismic seafloor deformation in the trench region during the Mw8.8 Maule megathrust earthquake. Sci. Rep. 7, srep45918. https://doi.org/10.1038/srep45918.

Masson, D.G., Parson, L.M., Milsom, J., Nichols, G., Sikumbang, N., Dwiyanto, B., Kallagher, H., 1990. Subduction of seamounts at the Java Trench: a view with long-range sidescan sonar. Tectonophysics 185, 51–65.

Métois, M., Vigny, C., Socquet, A., 2016. Interseismic coupling, megathrust earthquakes and seismic swarms along the Chilean subduction zone (38°–18°S). Pure Appl. Geophys. 173 (5), 1431–1449.

Noda, H., Lapusta, N., 2013. Stable creeping fault segments can become destructive as a result of dynamic weakening. Nature 493 (7433), 518.

Pritchard, M.E., Norabuena, E.O., Ji, C., Boroschek, R., Comte, D., Simons, M., Dixon, T.H., Rosen, P.A., 2007. Geodetic, teleseismic, and strong motion constraints on slip from recent southern Peru subduction zone earthquakes. J. Geophys. Res. 112, B03307. https://doi.org/10.1029/2006JB004294.

Ranero, C.R., Grevemeyer, I., Sahling, H., Barckhausen, U., Hensen, C., Wallmann, K., Weinrebe, W., Vannucchi, P., von Huene, R., McIntosh, K., 2008. Hydrogeological system of erosional convergent margins and its influence on tectonics and interplate seismogenesis. Geochem. Geophys. Geosyst. 9, Q03S04. https://doi.org/10.1029/2007GC001679.

Ranero, C.R., von Huene, R., 2000. Subduction erosion along the Middle America convergent margin. Nature 404, 748–752.

Ruiz, S., Metois, M., Fuenzalida, A., Ruiz, J., Leyton, F., Grandin, R., Vigny, C., Madariaga, R., Campos, J., 2014. Intense foreshocks and a slow slip event preceded the 2014 Iquique Mw 8.1 earthquake. Science. https://doi.org/10.1126/science.1256074.

Ryan, W.B.F., Carbotte, S.M., Coplan, J.O., O'Hara, S., Melkonian, A., Arko, R., Weissel, R.A., Ferrini, V., Goodwillie, A., Nitsche, F., Bonczkowski, J., Zemsky, R., 2009. Global multi-resolution topography synthesis. Geochem. Geophys. Geosyst. 10, Q03014. https://doi.org/10.1029/2008gc002332.

Saillard, M., Audin, L., Rousset, B., Avouac, J.-P., Chlieh, M., Hall, S.R., Husson, L., Farber, D.L., 2017. From the seismic cycle to long-term deformation: linking seismic coupling and Quaternary coastal geomorphology along the Andean megathrust. Tectonics 36, 2016TC004156. https://doi.org/10.1002/2016TC004156.

Schurr, B., Asch, G., Hainzl, S., Bedford, J., Hoechner, A., Palo, M., Wang, R., Moreno, M., Bartsch, M., Zhang, Y., Oncken, O., Tilmann, F., Dahm, T., Victor, P., Barrientos, S., Vilotte, J.-P., 2014. Gradual unlocking of plate boundary controlled initiation of the 2014 Iquique earthquake. Nature 512, 299–302. https://doi.org/10.1038/nature13681.

Schurr, B., Asch, G., Rosenau, M., Wang, R., Oncken, O., Barrientos, S., Salazar, P., Vilotte, J.P., 2012. The 2007 M7.7 Tocopilla northern Chile earthquake sequence: implications for along-strike and downdip rupture segmentation and megathrust frictional behavior. J. Geophys. Res. 117, B05305. https://doi.org/10.1029/2011jb009030.

Shirzaei, M., Bürgmann, R., Oncken, O., Walter, T.R., Victor, P., Ewiak, O., 2012. Response of forearc crustal faults to the megathrust earthquake cycle: InSAR evidence from Mejillones Peninsula, Northern Chile. Earth Planet. Sci. Lett. 333, 157–164.

Sibson, R.H., 1975. Generation of pseudotachylyte by ancient seismic faulting. Geophys. J. R. Astron. Soc. 43, 775–794. https://doi.org/10.1111/j.1365-246X.1975.tb06195.x.

Toda, S., Stein, R.S., Lin, J., 2011. Widespread seismicity excitation throughout central Japan following the 2011 M = 9.0 Tohoku earthquake and its interpretation by Coulomb stress transfer. Geophys. Res. Lett. 38, L00G03. https://doi.org/10.1029/2011gl047834.

Tsuji, T., Kawamura, K., Kanamatsu, T., Kasaya, T., Fujikura, K., Ito, Y., Tsuru, T., Kinoshita, M., 2013. Extension of continental crust by anelastic deformation during the 2011 Tohoku-Oki earthquake: the role of extensional faulting in the generation of a great tsunami. Earth Planet. Sci. Lett. 364, 44–58. https://doi.org/10.1016/j.epsl.2012.12.038.

Ujiie, K., Tanaka, H., Saito, T., Tsutsumi, A., Mori, J.J., Kameda, J., Scientists, E. 343 and 343T, 2013. Low coseismic shear stress on the Tohoku-Oki megathrust determined from laboratory experiments. Science 342 (6163), 1211–1214. https://doi.org/10.1126/science.1243485.

Vannucchi, P., Spagnuolo, E., Aretusini, S., Toro, G.D., Ujiie, K., Tsutsumi, A., Nielsen, S., 2017. Past seismic slip-to-the-trench recorded in Central America megathrust. Nat. Geosci. 10 (12), 935. https://doi.org/10.1038/s41561-017-0013-4.

Victor, P., Sobiesiak, M., Glodny, J., Nielsen, S.N., Oncken, O., 2011. Long-term persistence of subduction earthquake segment boundaries: evidence from Mejillones Peninsula, northern Chile. J. Geophys. Res., Solid Earth 116 (B2), B02402. https://doi.org/10.1029/2010JB007771.

von Huene, R., Ranero, C.R., 2003. Subduction erosion and basal friction along the sediment-starved convergent margin off Antofagasta, Chile. J. Geophys. Res. 108, 2079. https://doi.org/10.1029/2001JB001569.

Wang, K., Bilek, S.L., 2011. Do subducting seamounts generate or stop large earthquakes? Geology 39, 819–822. https://doi.org/10.1130/G31856.1.

Wang, K., Hu, Y., Huene, R., von Kukowski, N., 2010. Interplate earthquakes as a driver of shallow subduction erosion. Geology 38, 431–434. https://doi.org/10.1130/G30597.1.

Wang, K., Hu, Y., 2006. Accretionary prisms in subduction earthquake cycles: the theory of dynamic Coulomb wedge. J. Geophys. Res., Solid Earth 111 (B6), B06410. https://doi.org/10.1029/2005JB004094.